# COMPARISONS BETWEEN $2D+t$ POTENTIAL FLOW MODELS AND 3D RANS FOR PLANING HULL HYDRODYNAMICS

**A. Iafrati, R. Broglia**,
INSEAN (Italian Ship Model Basin), Rome, Italy,
E-mail: a.iafrati@insean.it, r.broglia@insean.it

## SUMMARY

The flow generated by a wedge shaped hull in steady planing motion is simulated numerically by a 2D+t potential flow model and by a 3D RANS solver. A comparison between the two solutions is established in order to understand the role played by three-dimensional effects, neglected within the slender body assumption. The analysis is focused on the evaluation of the free surface shape and of the pressure field acting on the hull surface. It is shown that a good agreement is achieved in terms of the free surface profile, provided a correction is applied to the 2D+t solution to account for the rise up of the water in front of the hull. The comparison in terms of pressure distribution reveals important three-dimensional effects in the very fore part of the hull, in the region about the separation point and at the transom.

## 1. INTRODUCTION

The motivation for the study stems from the fact that, differently from displacement ships where computational methods have reached a high level of confidence, not so much has been done for planing crafts. In this case the development of numerical tools has been hampered by the much stronger role played by nonlinear effects and by the smallness of the scales that have to be resolved in order to achieve an accurate prediction of the pressure field, particularly in the fore region. Because of such limitations, most of the theoretical or numerical studies have been developed under the slender body assumption (Tulin, 1956; Savander, 1997; Zhao, Faltinsen and Haslum, 1997; among others) and only few attempts were made to face the full three-dimensional problem (Lai and Troesch, 1995; 1996). By exploiting the slenderness of the body, the flow generated by a planing hull in steady motion on a transversal plane in an earth fixed frame of reference can be approximated by that induced by the water entry of a two-dimensional body. This approach, which is known as 2D+t, has been used for instance by Battistin and Iafrati (2003*a*) to model the flow generated by hulls in steady motion whereas Sun and Faltinsen (2007) initiated the extention of the approach to seakeeping problems. Generally, the shape of the two-dimensional impacting body changes in time as it represents the hull section at different longitudinal positions. This is not the case for the present paper as the hull is wedge shaped.

Despite the awareness of the limits of the slender body assumption, no specific studies have been done so far to achieve a quantitative estimate of the neglected three-dimensional effects. Although still rather expensive, RANS flow solvers have reached a good level of development and are now capable of providing accurate solutions, provided the grid resolution is fine enough to capture the sharp gradients taking place in the fore part of the hull especially.

Starting from the above considerations, a comparison is presented here between the 2D+t potential flow solution and the RANS results. As a test case, the flow generated by a wedge shaped planing hull moving steadily is considered. The cross section of the hull has a 20 degrees deadrise angle whereas the trim angle is fixed at 4 a 6 degrees. Such conditions have been chosen as experimental data ara available (Kaprian and Boyd, 1955). The 2D+t model uses a fully nonlinear, potential flow solver to derive the solution of the Laplace equation for the velocity potential. Simulations are carried out in the infinite Froude number limit, which is to say that the hydrostatic contribution to the pressure has been neglected in comparison to nonlinear terms. This hypothesis avoids that the jet, detaching from the chine, plunges onto the free surface, leading to a topology change that would be hardly managed by the boundary element model.

Results are presented in terms of free surface profiles at different longitudinal positions and pressure distributions on the hull surface. Due to limitation in space, results are here presented for the 6 degree cases only. More results will be presented at the workshop. At the workshop, comparisons with other numerical results available in literature and experimental measurements will be presented as well.

## 2. $2D+t$ POTENTIAL FLOW MODEL

Without going into a detailed formulation of the model, which can be found in Zhao, Faltinsen and Haslum (1997) or in Battistin and Iafrati (2003*a*), for the purpose of the present paper it is enough to recall that the steady three-dimensional flow is transformed in the unsteady two-dimensional water entry flow taking place on the $y, z$ plane located at $x = 0$ (Fig. 1,2):

$$\frac{\partial^2\varphi}{\partial y^2} + \frac{\partial^2\varphi}{\partial z^2} = 0 \qquad (\Omega) \tag{1}$$

$$\frac{\partial\varphi}{\partial n} = -U_H \frac{\nu_x}{\sqrt{1-\nu_x^2}} \qquad (S_B) \tag{2}$$

$$\frac{\partial h}{\partial t} + \boldsymbol{u}\cdot\nabla h = 0 \qquad (S_S) \tag{3}$$

$$\frac{\partial\varphi}{\partial t} + \boldsymbol{u}\cdot\nabla\varphi = \frac{|\boldsymbol{u}|^2}{2} \qquad (S_S) \tag{4}$$

$$\varphi(0,y,0,0) = 0 \qquad (S_S) \tag{5}$$

$$F(y,0,0) = 0 \quad (S_S)\ . \tag{6}$$

Here $U_H$ is the horizontal speed of the hull and $\boldsymbol{n}$ is the normal to the two-dimensional hull section $S_B$, which is obtained by re-normalizing the projection of the three-dimensional normal $\boldsymbol{\nu}$ onto the $x = 0$ plane. Correspondingly, in the two-dimensional problem $\boldsymbol{u}$ is the projection of the three-

dimensional velocity vector onto the same plane. In the above equations $\nabla = (\partial_y, \partial_z)$ is the two-dimensional gradient operator, whereas $F(y, z, t)$ is the equation of the free surface $S_S$.

The initial boundary value problem in the two-dimensional plane is solved through a mixed Eulerian-Lagrangian technique (Battistin and Iafrati, 2003*b*) and the corresponding pressure field along the wetted portion of the contour is evaluated by the unsteady Bernoulli equation

$$p = -\left(\varphi_t + \frac{|\nabla\varphi|^2}{2}\right). \tag{7}$$

where $\rho_0 U_H^2$ is the scaling factor, $\rho_0$ being the fluid density.

The solution of the boundary value problem is achieved through a boundary element approach. The fluid boundary is discretized with straight line panels, and the velocity potential and its normal derivative are assumed to be piecewise constant. The system is integrated in time making use of a second-order Runge-Kutta scheme. For stability reasons, the time step is chosen so that the maximum displacement of the centroid is smaller than one fourth of the corresponding panel length. The geometry of the impacting body is given through a set of points, which are interpolated with cubic splines.

Although a more detailed description of the numerical model can be found in Iafrati and Battistin (2003), it is worth spending few words describing the method adopted to describe some peculiarities in the flow features, which are the thin jet layer and the flow separation taking place in the chine wetted region. Even two-dimensional simulations are rather challenging because of the thin jet layer developing along the body contour. Despite the rather low pressure inside the jet, the description of the spray is important in order to obtain a correct estimate of the wetted surface and of the flow separation point. A hybrid FEM-BEM simplified model has been proposed in Battistin and Iafrati (2004). In this simplified model the jet is subdivided into small control volumes and within each volume the velocity potential is written in the form of an harmonic Taylor series, up to the second order. The coefficients of the expansion are derived together with the solution of the boundary value problem. An intermediate region is introduced to assure a smooth transition from the bulk of the fluid to the jet region. More details concerning with the parameters governing the modelled part of the jet are given in Iafrati and Battistin (2003) and Battistin and Iafrati (2004).

The occurrence of flow separation from the body contour during the impact is included in the present model, at least for those cases in which the separation point can be assigned *a priori*, as it is for the present geometry. It is assumed that, when the jet tip reaches the separation point, the liquid particles which were moving along the body contour, continue moving along the tangent to the body at the separation point. Although very close to the separation point a Neumann boundary condition is enforced on the free surface to guarantee the tangency to the body contour, further away on the separated part the standard kinematic and dynamic boundary conditions hold, thus providing a Dirichlet boundary condition for the velocity potential. Once the fluid leaves the body, the jet model is simplified further, by reducing the series expansion to the first order. Although this assumption does not allow an exact mass conservation in the jet region, it greatly improves the stability of the numerical algorithm.

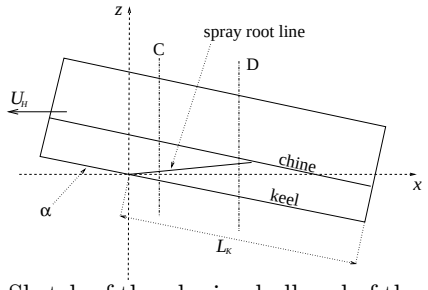


Figure 1: Sketch of the planing hull and of the notation employed

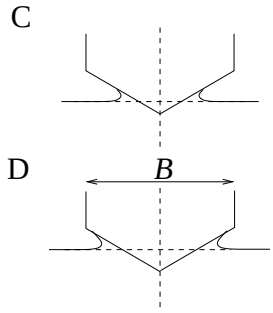


Figure 2: Sketch of the flow in the transversal plane

## 3. RANS FLOW SOLVER

The three-dimensional RANS solutions are obtained by using the method described in Di Mascio, Broglia and Muscari (2007). The method solves the unsteady Reynolds Averaged Navier-Stokes equations for an incompressible fluid, which are written in non-dimensional integral form with respect to a moving control volume $\mathcal{V}$ as

$$\begin{gathered} \oint_{S(\mathcal{V})} \boldsymbol{U}\cdot\boldsymbol{n}\mathrm{d}S = 0 \\ \frac{\partial}{\partial t}\int_{\mathcal{V}} \boldsymbol{U}\mathrm{d}V + \oint_{S(\mathcal{V})} (\mathcal{F}_c - \mathcal{F}_d)\cdot\boldsymbol{n}\mathrm{d}S = 0 \end{gathered} \tag{8}$$

where $S(\mathcal{V})$ is the boundary of the control volume, and $\boldsymbol{n}$ the outward unit normal. In equation (8), $\mathcal{F}_c$ and $\mathcal{F}_d$ represent Eulerian (advection and pressure) and diffusive fluxes, respectively:

$$\begin{aligned} \mathcal{F}_c &= p\mathbf{I} + (\boldsymbol{U}-\boldsymbol{V})\,\boldsymbol{U} \\ \mathcal{F}_d &= \left(\frac{1}{Rn} + \nu_t\right)\left[\mathrm{grad}\boldsymbol{U} + (\mathrm{grad}\boldsymbol{U})^{\mathrm{T}}\right] \end{aligned} \tag{9}$$

where $\boldsymbol{V}$ is the local velocity of the boundary of the control volume, $Rn = U_\infty L/\nu$ the Reynolds number, $\nu$ the kinematic viscosity, whereas $\nu_t$ denotes the non–dimensional turbulent viscosity. The latter is calculated by the one–equation model introduced by Spalart and Allmaras (1994). In the above equations, $u_i$ is the $i$–th Cartesian component of the velocity vector, $p$ is a variable related to the pressure $P$ and the acceleration of gravity $g$ (parallel to the vertical axis $z$, downward oriented) by $p = P + z/Fn^2$,

$Fn = U_\infty/\sqrt{gL}$ being the Froude number. The system of equations (8) is solved under appropriate conditions at physical and computational boundaries. On solid walls, the relative velocity is set to zero whereas pressure is not required. At the inflow boundary of the computational domain, velocity is set to the undisturbed flow value and the pressure is extrapolated from inside. The pressure is set to zero at the outflow boundary, where velocity components are extrapolated from inside.

At the free surface, location of which is one of the unknowns of the problem, the dynamic boundary condition requires continuity of stresses. In the present paper the presence of air is neglected so that the continuity of stresses at the interface read

$$\begin{aligned} p &= \tau_{ij} n_i n_j + \tfrac{z}{Fn^2} + \tfrac{\kappa}{We^2} \\ \tau_{ij} n_i t^1_j &= 0 \\ \tau_{ij} n_i t^2_j &= 0 \end{aligned} \qquad (10)$$

where $\tau_{ij}$ is the stress tensor, $\kappa$ is the average curvature, $We = \sqrt{\rho U^2_\infty L/\sigma}$ is the Weber number, $\sigma$ being the surface tension coefficient. In the above equation $\boldsymbol{n}$, $\boldsymbol{t}^1$ and $\boldsymbol{t}^2$ are the surface normal and two tangential unit vectors, respectively. The method is second order accurate in space and time and uses a single phase Level-Set technique to describe the free surface dynamics.

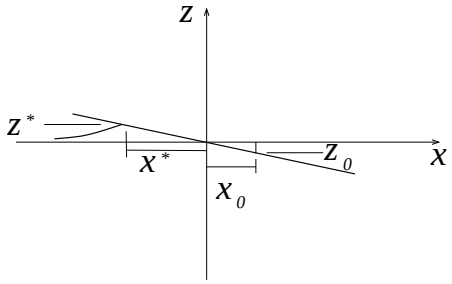


Figure 4: Limits of the $2D+t$ model: $z^*$ and $x^*$ locate the intersection point between the free surface and the keel line whereas $z_0$ is the initial depth of the apex in the $2D+t$ simulations.

## 4. NUMERICAL RESULTS

Numerical simulations are carried out for a wedge shaped planing hull, 20 degrees deadrise angle, planing with a constant trim angle of 4 and 6 degrees (only results for the 6 degrees case are shown here). The hull beam $B$ is assumed as length scale. The hull, which is $4B$ long, is rotated about the quarter of length yielding to a geometrical wetted length $L_K = 3B$. Whereas potential flow simulations are carried out in the infinite Froude number limit, RANS simulations are performed at a beam Froude number $Fr_B = U/\sqrt{gB} = 12.25$. Before establishing the comparison, it is important to remark two limitations in the $2D+t$ solution which have to properly accounter for. Due to the lack of three-dimensional effects at the bow, the $2D+t$ solution cannot predict the rise up of the water level in the very fore part of the hull. Furthermore, in the $2D+t$ approach, the wedge is slightly submerged at the beginning of the simulation.

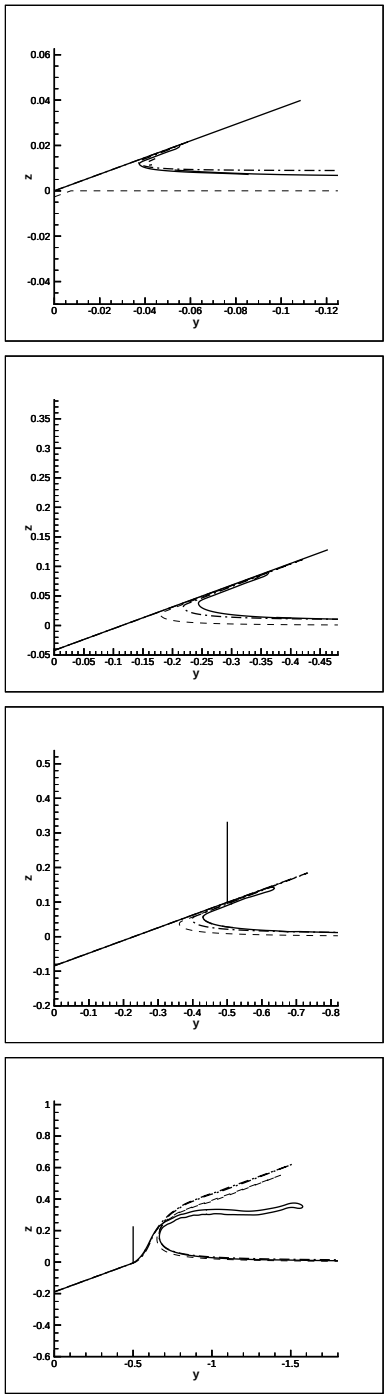


Figure 5: Comparisons between the free surface shapes provided by the three-dimensional RANS (*solid*) and the $2D+t$ model (*dash*). For the latter, profiles obtained after correction are also displayed (*dash-dot*). From top to bottom, results refer to the 6 degrees trim angle at $x = 0, 0.4, 0.8, 1.8$.

Although the initial submergence can be reduced, it cannot be completely avoided. In order to account for the above effects and thus to establish a fairer comparison, the three-dimensional solution at the longitudinal position $x$ is compared with the $2D+t$ solution obtained at the same position and at a position $\tilde{x} = x + (x_0 - x^*)$ (see Fig. 3). For the conditions adopted in the present calculations, $x^* \simeq -0.0588$ for the 4 and 6 degrees trim angle. Of course, when the horizontal shift is applied, a vertical displacement is also introduced in order to the have the body located at the same

vertical position of the three-dimensional solution.

In Figs. 5 and 6, comparisons between the $2D + t$ and the RANS solutions are established in terms of free surface shape and pressure distribution, respectively.

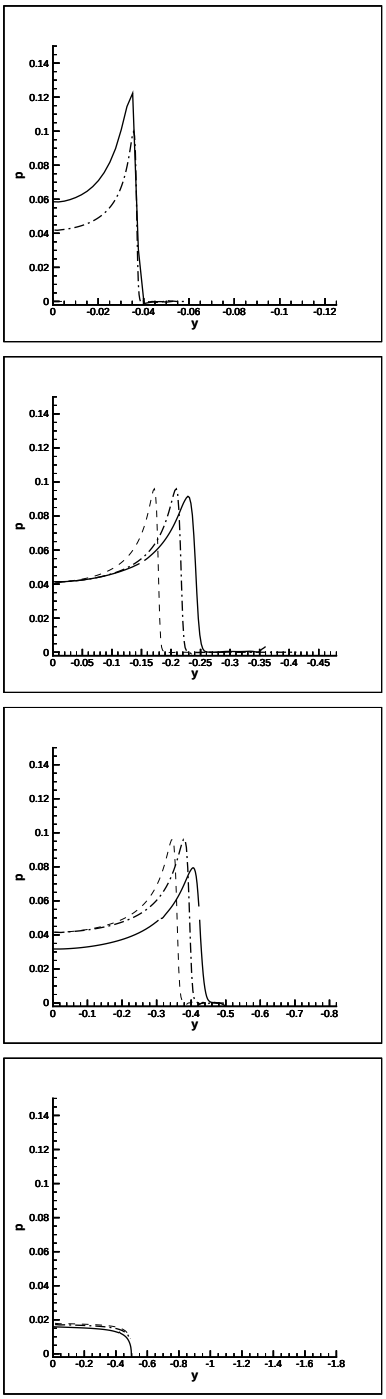


Figure 6: Comparisons between the pressure distribution of the body surface for the 6 degrees trim angle. From top to bottom, results refer to the transversal planes located at $x = 0, 0.4, 0.8, 1.8$.

The comparison indicates that the $2D + t$ and three-dimensional results are in a rather good agreement in terms of the free surface dynamics, provided the correction accounting for the rise up of the water for the initial body depth is applied. It is worth noticing that, despite the lack of gravity in the $2D + t$ simulations, the agreement remains very satisfactory even in the chine wetted phase. Comparisons (not shown here) of free surface profiles further downstream show that, although the gravity is starting to act on the thinnest part of the jet, the solution up to the jet root is well captured by the $2D + t$ simulation, in spite of the zero gravity assumption.

Differently from the free surface shape, the comparison in terms of pressure distribution is satisfactory only in the chine un-wetted stage, which is up to $x = 0.6$ for 6 degrees case. Owing to the lack of the longitudinal derivative, the $2D+t$ solution exhibits a much sharper variation in the pressure field about the region where the flow separates from the bottom of the hull. Further downstream, the agreement becomes again satisfactory (Fig. 6, x=1.8). Approaching the transom, the three-dimensional solution exhibit a smooth reduction of the pressure which is not predicted by the $2D+t$ solution.

## 5. REFERENCES


D. Battistin and A. Iafrati (2003*a*) *A numerical model for hydrodynamics of planing surfaces*, FAST 2003, Ischia, IT.

D. Battistin and A. Iafrati (2003*b*) *Hydrodynamic loads during water entry of two-dimensional and axisymmetric bodies*, J. Fluids and Struct., Vol. 17, p. 643.

D. Battistin and A. Iafrati (2004) *A numerical model for the jet flow generated by water impact*, J. Engng Math., Vol. 48, p. 353.

A. Di Mascio, R. Broglia and R. Muscari (2007) *On the Application of the Single–Phase Level Set Method for Naval Hydrodynamic Flows*, Comp. and Fluids, Vol. 36(5), p. 868.

A. Iafrati and D. Battistin (2003) *Hydrodynamics of Water Entry in Presence of Flow Separation from Chines*, Proc. $8^{th}$ NSH Conf., Busan, KR.

W.J. Kaprian and G.M. Boyd Jr. (1955) *Hydrodynamic pressure distribution obtained during a planing investigation of vive related planing surface*, Tech. Report, TN 3477, NACA.

C. Lai and A.W. Troesch (1995) *Modeling issues related to the hydrodynamics of three-dimensional steady planing*, J. Ship Res., Vol. 39, p. 1.

C. Lai and A.W. Troesch (1996) *A vortex lattice method for high speed planing*, Int. J. Num. Meth. Fluids, Vol. 22, p. 495.

B.R. Savander (1997) *Planing hull hydrodynamics*, PhD thesis, Dept. NAME, Univ. Michigan, Ann Arbor (MI), US.

P.R. Spalart and S.R. Allmaras (1994) *A One–Equation Turbulence Model for Aerodynamic Flows*, Recherche Aérospatiale, Vol. 1, p. 5.

H. Sun and O.M. Faltinsen (2007) *Hydrodynamic forces on a planing hull in forced heave or pitch motions in calm water*, Proc. $22^{nd}$ IWWWFB, Plitvice, HR.

M.P. Tulin (1956) *The theory of slender surfaces planing at high speed*, Schiffstechnik, Vol. 4, p. 125.

R. Zhao, O.M. Faltinsen and H. Haslum (1997) *A simplified nonlinear analysis of a high speed planing craft in calm water*, FAST '97, Sydney, p. 431.